Tunable Fano resonances and plasmonic hybridization of gold triangle–rod dimer nanostructure*

Meng Huang(黄萌)[1,†], Dong Chen(陈栋)[2], Li Zhang(张利)[2], and Jun Zhou(周骏)[2]

[1] College of Electrical and Information Engineering, Quzhou University, Quzhou 324000, China
[2] Institute of Photonics, Faculty of Science, Ningbo University, Ningbo 315211, China

(Received 10 November 2015; revised manuscript received 13 January 2016; published online 31 March 2016)

A gold dimer structure consisting of a notched triangle nanoslice and a rectangle nanorod is proposed to produce distinct Fano resonance. Owing to the coupling between the dipole plasmon mode of the nanorod and the dipole or quadrupole plasmon mode of the nanoslice, the extinction spectrum with a deep Fano dip is formed and can be well fitted by the Fano interference model for different geometry parameters. In addition, Fano resonance of the gold dimer nanostructure also intensely depends on the polarization direction of incident light. Moreover, Fano resonance of the triangle–rod trimer is also analyzed by adding another nanorod into the former dimer and exhibits the splitting of plasmonic resonant peak in high order coupling modes. The plasmonic hybridizations in these nanostructures have been analyzed for revealing the physical origin of the Fano resonance.

Keywords: surface plasmon, Fano resonance, dimer, trimer

PACS: 73.20.Mf, 52.35.Mw, 87.85.fk **DOI:** 10.1088/1674-1056/25/5/057303

1. Introduction

As is well known, the optical properties of noble metallic nanostructures are dominated by the excited localized surface plasmon resonance (LSPR) when the frequency of the incident electromagnetic wave is virtually identical to the vibration frequency of collective electron in the nanostructure.[1] The frequency, strength, and quality of the LSPR depend on the size, geometry, and composition of an individual metallic nanostructure, and also relate to the refractive index of the local environment.[2–4] In particular, the LSPR characteristic of a metal nanoparticle is intensively sensitive to the presence of other nearby metal nanoparticles. When two LSPR bands are overlapped and coupled through near-field interactions, splitting of the modal energies can occur and the bonding and antibonding modes are formed according to the plasmon hybridization theory.[5] Thence, for obtaining tunable richer plasmonic features, not only metallic nanostructures with different shapes such as spheres,[6] rods,[7] rings,[8,9] disks,[10] cube,[11] and shells,[12–14] but also the complex nanostructures with two or more elementary metallic shapes have been theoretically and experimentally investigated.[15–18] As a typical example, Fano resonance of a metallic nanostructure with complex or asymmetric geometry has become a research focus.[19–21] In fact, Fano resonance is caused by the interactions of a broad "bright" plasmon mode and a relatively narrow "dark" plasmon mode in metallic nanostructure and exhibits an asymmetric extinction line shape, and the feature of Fano resonance is highly sensitive to the geometric parameters of nanostructure, the angle of incidence light and the dielectric permittivity of environment,[22–24] so that a small perturbation can induce the dramatic shift of resonance lineshape. It is the above property to render many promising advantages of Fano resonance in actual applications such as chemical or biological sensors,[25] electromagnetically induced transparency (EIT),[26] switching,[27] plasmonic nanolasing,[28] and slow light.[29]

In recent years, besides the simple dimer nanostructures including sphere–sphere dimer,[30] sphere–rod dimer,[31] rod–rod dimer,[32] rod–ring disks dimer,[33–35] the plasmonic properties of other symmetry-breaking dimers[36] and the heterodimers composed of silver, gold, and copper nanoparticles have been widely studied because of their outstanding advantages of tunable plasmon resonance which intensely depend on polarization angles of incident light, gap of interparticle separations, especially, their multipolar Fano features are easily excited by hybridizing of a bonding quadrupole–quadrupole mode and a dipole–quadrupole mode.[37] For example, the plasmonic responses (including Fano resonances) of heterodimers with an Au nanorod and a small Au nanosphere, are remarkably sensitive to the nanosphere position on the nanorod, the gap distance, and the nanocrystal dimensions. As the nanosphere is moved around the nanorod, the rotational symmetry of the Au nanorod–nanosphere heterodimer is broken, which causes the coupling of plasmon modes and the varying of Fano interference.[31] The Fano resonance of T-shaped nanorod dimer or angle–resolved nanorod dimer can

*Project supported by the National Natural Science Foundation of China (Grant No. 61275153) and the Natural Science Foundation of Zhejiang Provice, China (Grant No. LY12A04002).

†Corresponding author. E-mail: xdxhuang@163.com

© 2016 Chinese Physical Society and IOP Publishing Ltd

induce two splitting hybridized bonding and antibonding resonance modes which are affected by the geometry parameters and the incident polarization.[32] Yang *et al.* reported that the Fano resonance in gold ring–rod nanocavities with more than one nanorod, i.e., the plasmon coupling in the theta-shaped ring–rod cavity exhibits a flexible tunability.[34] Meanwhile, the narrow and deep Fano dip in LSPR spectrum can be achieved in the nanostructures with a rod and concentric square ring-disk.[35] The extinction properties of a plasmonic nanocavity consisting of a regular triangle embedded in a split ring are also sensitive to the polarization of the incident light, which results in strong Fano resonances.[36] Therefore, it is interesting to pay attention on the Fano resonances of the dimer with special shaped metal nanostructure.

In this paper, we design a gold dimer consisting of a notched triangle nanoslice and a cuboid nanorod to produce strong Fano resonances. The Fano resonances of gold dimer are formed by the plasmonic coupling between the "bright" dipole mode of the nanorod and "bright" dipole or the "dark" quadrupole modes of nanoslice, respectively. By using the Fano interference model and finite element method (FEM), the effects of the structure parameters and the incident polarization on the Fano resonances are analyzed for understanding the underlying physics of the Fano resonances in this dimer. In addition, compared with the works described above, the split of Fano resonance profile can be easily formed by simply extending the dimer to a trimer with another cuboid nanorod and used as a multi-wavelength high sensitive sensor in the near-infrared region.

2. Dimer structure and simulation method

The schematic graph of the proposed gold triangle–rod dimer nanostructure is plotted in Fig. 1, in which the notched triangle nanoslice is a regular triangle with equilateral triangle split and the nanorod is in the shape of a rectangle. In Fig. 1, all the geometry parameters are in nano-dimensions and can be easily fabricated by the electron beam lithography (EBL) technology.[38] The thicknesses of the notched triangle nanoslice and the rectangle nanorod are the same and labeled as H; the side length of the nanoslice is L_1, the side length of the equilateral triangle split S equals to $L_1/3$ and its vertex at the geometric center of the nanoslice; the edge length and width of the nanorod are L_2 and W, respectively. As shown in Fig. 1(b), the proposed dimer is designed into a special assembly in which the nanorod is fixed toward a bevel side of the nanoslice at a gap d and a geometric center separation of the nanoslice and nanorod g. The plane electromagnetic wave is incident on the dimer along the z direction with x polarization. The permittivity data of gold are obtained from the experimental results of Johnson and Christy,[39] and the dimer is assumed to be immersed in the air.

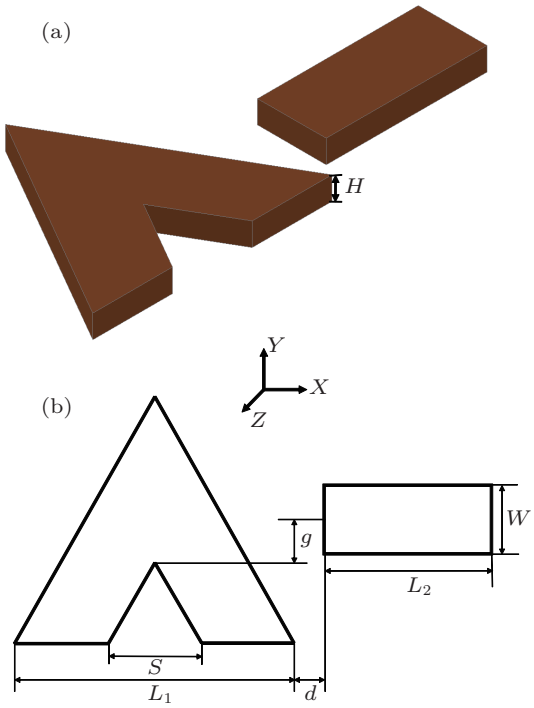


Fig. 1. (color online) (a) Model configuration of the proposed dimer and (b) geometric parameters of the notched triangle nanoslice and the rectangle nanorod: $L_1 = 130$ nm, $L_2 = 120$ nm, $W = 60$ nm, $H = 30$ nm, $S = L_1/3 = 43.3$ nm.

By using the scattering field formulation, the optical properties of the proposed gold triangle–rod nanostructure can be numerically studied in the frequency domain and be well expressed by the scattering cross-section ($C_{\rm scat}$), the absorption cross-section ($C_{\rm abs}$), and the extinction cross-section ($C_{\rm ext}$), respectively. That is that $C_{\rm scat}$ is obtained by integrating the normalized electric field around a far-field transform boundary enclosing the dimer. Similarly, $C_{\rm abs}$ is obtained by integrating the time-average resistive heating ($U_{\rm av}$). Here, $C_{\rm scat}$ and $C_{\rm abs}$ are expressed as follows:[40]

$$C_{\rm scat} = \frac{1}{|E_{\rm inc}|^2}\int |E_{\rm far}|^2 \,{\rm d}S, \tag{1}$$

$$C_{\rm abs} = \frac{2}{\sqrt{\varepsilon_0/\mu_0}|E_{\rm inc}|^2}\int U_{\rm av}\,{\rm d}V, \tag{2}$$

where $E_{\rm inc}$ is the incident electric field, $E_{\rm far}$ is the far-field electric component of the scattering field calculated by the Stratton–Chu formula,[40] ε_0 and μ_0 are vacuum permittivity and vacuum permeability, respectively. In addition, $U_{\rm av} = 1/2\,{\rm Re}(\sigma E\cdot E^* - {\rm j}\omega \boldsymbol{E}\cdot\boldsymbol{D}^*)$, σ is the conductivity of gold, $\boldsymbol{E}$, $\boldsymbol{D}$, and ω are electric field vector, electric displacement vector, and angular frequency of the incident light, respectively.

In fact, the extinction cross-section $C_{\rm ext}$ of the system is defined as the total radiation flux of scattering and absorption transmitting through the system. We have

$$C_{\rm ext} = C_{\rm scat} + C_{\rm abs}. \tag{3}$$

In our research, the commercial software package COMSOL Multiphysics 4.3 incorporated RF module, which con-

tains electromagnetic scattering formula code based on the three-dimensional finite element method (3D-FEM), was used to calculate the extinction cross section, near-field intensity distributions, and charge distributions. As we know, FEM is an effective research method of the near-field optics and suitable to analyze the optical properties of metallic nanostructures. It is said that the electromagnetic problems of complex nanostructures can be effectively handled by solving Maxwell's equations on an appropriate discretized spatial grid.[41,42] In our numerical simulations, the perfectly matched layers were used in the propagation direction to eliminate the nonphysical reflections at the domain boundaries, and the triangle–rod dimer nanostructure was meshed with tetrahedral elements and a local mesh refinement was used in and around the dimer.

3. Results and discussion

For the different polarizations of incident light, the extinction cross-section spectra of the individual notched triangle nanoslice and nanorod are shown in Fig. 2(a), and the electric field distributions of nanoslice and nanorod at the wavelengths of all resonant peaks are shown in Fig. 2. As shown in Fig. 2(a), the dipole resonance peaks of nanorod and nanoslice are located at 680 nm and 780 nm, respectively, which are broad modes excited by incident light polarized along the horizontal direction. Whereas for the incident light polarized along the vertical direction, the quadrupole mode of the nanoslice is located at 680 nm, the resonance peak corresponding to the octupolar mode of the nanoslice is located at 630 nm. It is clear that there is a large gap between the extinction spectra of the nanorod and the nanoslice, that is, an intense coupling among their plasmon modes, if the nanorod and the nanoslice are combined into a dimer. Therefore, it is expected that the dimer nanostructure could result in a distinct Fano resonance due to the strong interaction of the plasmon modes including the dipole mode of the nanorod and the dipole/quadrupole modes of the notched triangle nanoslice.

Factually, for the case of the polarization of incident light along the horizontal direction, the dipole plasmon modes in the nanoslice and the nanorod are excited into bright modes with lower energies. The quadrupole plasmon mode in the nanoslice cannot be excited as a dark mode in the far field by the horizontal polarization light, but it can be excited effectively by the near-field plasmon coupling between the dipole mode of the nanorod and the quadrupole of the nanoslice. By bringing the nanorod and nanoslice close to each other, the bright dipole mode of nanorod and the dark quadrupole mode of the nanoslice can overlap and destructively interfere at the resonant wavelength to form an Fano dip in the extinction spectrum.

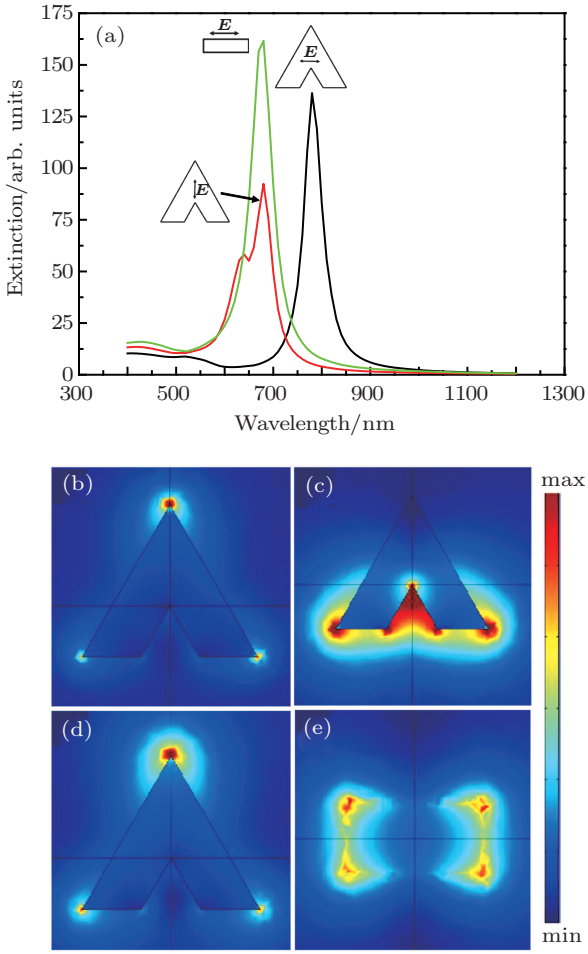


Fig. 2. (a) Extinction spectra of the individual gold nanorod and a notched triangle nanoslice. Here, $\boldsymbol{E}$ shows the polarization of the electric field, and the propagation direction of plane wave is along $-z$ axis. The electric field distributions of the individual notched triangle nanoslice for the resonant peaks at (b) 630 nm, (c) 680 nm, (d) 720 nm, respectively. (e) The electric field distributions of individual gold nanorod for the resonant peaks at 680 nm.

On the other hand, it is important to discuss the lineshape feature of Fano resonance and the electric field distributions of the dimer nanostructure. Figure 3(a) gives the extinction spectrum of the triangle–rod dimer nanostructure with a geometric center separation of $g = 0$ nm and a gap distance of $d = 2$ nm for the horizontal polarization of the incident light. As shown in Fig. 3(a), one Fano dip and two plasmonic peaks are located at 720 nm, 660 nm, and 860 nm, respectively. From the viewpoint of plasmon hybridization, the resonant coupling between the plasmon modes of individual nanostructures in the dimer can lead to the splitting of their modes into a bonding plasmon mode and a antibonding plasmon mode. In our case, the low-energy bonding plasmon mode located at 860 nm is raised from the interaction of the dipole–dipole plasmonic modes of the notched triangular nanoslice and the rectangular nanorod, while the high-energy antibonding plasmon mode located at 660 nm from the coupling of their dipole–quadrupole plasmon modes. The intensity of the antibonding plasmon mode in the Fano resonant spectrum is much weaker than that of the bonding plasmon mode due to the weak coupling between the

dipole mode of the nanorod and the quadrupole mode of the nanoslice. In order to better understand the physical origin of the extinction spectra, the charge and electric field distributions of the dimer structure are shown in Figs. 3(b)–3(g) for three wavelengths of incident lights, respectively. Comparing Fig. 3(b) with Figs. 3(c) and 3(d), we find that the charge distributions of the nanorod have almost opposite signs, but the charge distributions of the nanoslice display the same or opposite signs in a different area. Specifically, we can see from Figs. 3(e)–3(g), the electric fields locate in the gap between the nanoslice and the nanorod and the low edge of the triangle nanoslice is gradually enhanced and reached a maximum at the resonant wavelength of 860 nm due to the strong coupling of the dipole mode of the nanorod and the dipole mode of the nanoslice. It is the strong coupling of dipole–dipole and dipole–quadrupole modes in the triangle–rod dimer nanostructure that Fano interference is formed into a perfect profile with a deep dip and a narrow line width.

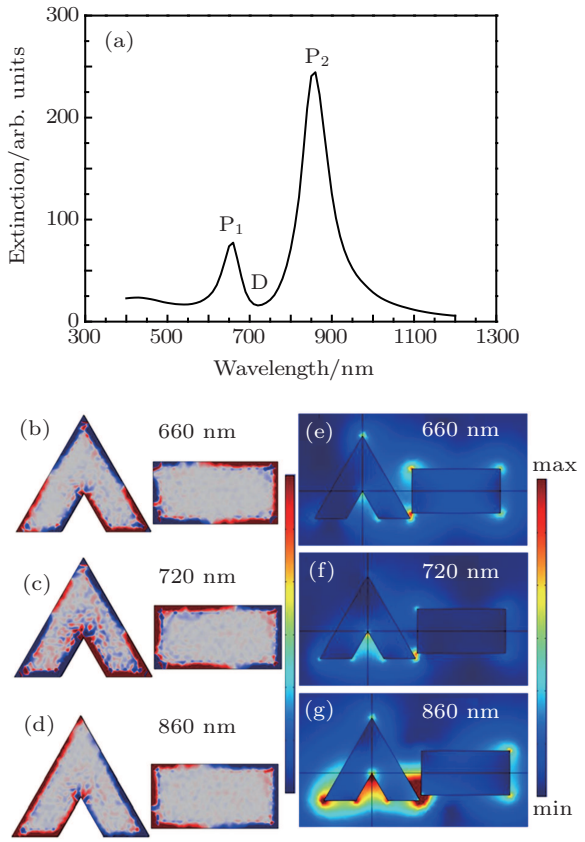


Fig. 3. (color online) (a) Extinction spectrum of the triangle–rod dimer nanostructure with a geometric center separation $g = 0$ nm and a gap distance $d = 2$ nm; (b)–(d) The charge distributions at the Fano peak P_1, Fano dip D, Fano peak P_2, respectively; (e)–(g) The electric field distributions at Fano peak P_1, Fano dip D, Fano peak P_2, respectively.

Furthermore, the Fano resonance characteristic of the proposed dimer can be tuned by adjusting the geometry of the triangle–rod nanostructure. Figure 4 shows the extinction spectra of the dimer with varying the center offset g and the gap distance d. There are three phenomena that can be seen from Fig. 4(a). Firstly, the peak wavelengths of the low-energy bonding plasmon modes red-shift with the decrease of g, but the peak wavelengths of the high-energy antibonding plasmon mode blue-shift with the decrease of g. The reason is that the interactions between the bright dipole mode and the dark quadrupole mode are enhanced with the decrease of g, which give rise to a large energy gap between the antibonding and bonding modes and make the peak position of antibonding mode to be blue-shifted and the peak position of bonding mode to be red-shifted. Secondly, the resonance intensities of high-energy antibonding plasmon modes are weaker and weaker with the decrease of g. It could be attributed to the weak coupling between the quadrupole plasmon mode of nanoslice and the dipole plasmon mode of nanorod with the decrease of g due to the enhanced electric-fields being focused on the front angle of the nanoslice as shown in Fig. 3(e). On the contrary, the resonance intensities of the low-energy bonding plasmon modes are stronger and stronger with the decrease of g due to the enhanced electric-field being focused on the split side of the nanoslice as shown in Fig. 3(g). Thirdly, the Fano dip gets deeper with the decrease of g because of the intense coupling between the super-radiative dipolar mode of nanorod and the super-radiative dipole mode or subradiative quadrupole mode of the nanoslice. In addition, as shown in Fig. 4(b), the separation of resonant peaks between the high-energy antibonding plasmon modes and the low-energy bonding plasmon modes decreases with the increase of d, also the Fano dip gets shallower. This effect is determined by the weak coupling between the super-radiative dipole mode of the nanorod and the dipole or quadrupole modes of the nanoslice due to the increase of coupling distance. Comparing Fig. 4(a) with Fig. 4(b), it is interesting to find that the Fano resonances of the dimer depend inversely on the geometric parameters g and d.

The Fano resonance characteristic of the proposed dimer is also dependent on the polarization direction of incident light. As shown in Fig. 5, when the polarization angle $\theta = 0°$, the extinction spectra with a single Fano dip is formed, while for $\theta = 90°$, only one resonant peak around 700 nm corresponding to the quadrupole mode of the nanoslice is formed, that is, Fano resonance disappears. As explained above, this is attributed to the fact that the Fano resonance can be effectively excited by only E_x component of incident light for $\theta = 0°$ due to the interaction between the dipole and the quadrupole modes. However, when $\theta = 90°$, only the E_y component exists, leading to the quadrupole mode of the nanoslice being effectively excited and the dipole mode of the nanorod cannot be excited. As is also shown in Fig. 5, when $\theta = 45°$ and 60°, the imperfect Fano resonances are formed due to the interactions among the dipole mode of the nanorod and the dipole/quadrupole modes of the nanoslice, which are induced by the E_x and E_y components of the incident light. It is clear

that the Fano resonance gradually weakens till it disappears with the increase of polarization angle of incident light, accompanying the process from an intense coupling to a weak coupling between the excited dipole mode of the nanorod and the quadrupole mode of the nanoslice.

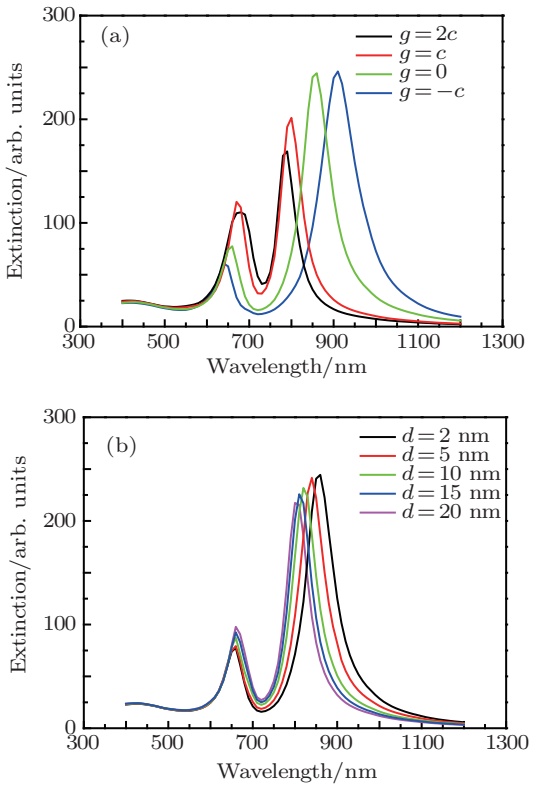


Fig. 4. (a) Extinction spectra of the triangle–rod dimer nanostructure with varying the center offset g for the fixed gap distance $d = 2$ nm; (b) extinction spectra of the triangle–rod dimer nanostructure with varying the gap distance d and the fixed center offset $g = 0$ nm. The constant c equals to the vertical distance between the center and the side of notched triangle nanoslice.

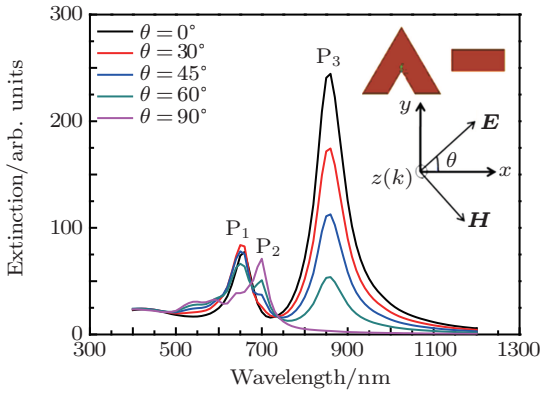


Fig. 5. The incident polarization effects on the extinction spectra of the triangle–rod dimer nanostructure ($g = 0$ nm, $d = 2$ nm). The inset shows incident polarizations.

It is more interesting that the extinction spectrum of the triangle–rod trimer nanostructure demonstrates the perfect profile of Fano resonance. The triangle–rod trimer consists of two nanorods and a notched triangle nanoslice and is drawn in Fig. 6. Figure 7 gives the extinction spectrum of the trimer with a symmetric structure. It is obvious that the profile of Fano resonant of the trimer exhibits a more perfect lineshape with a more intense resonance peak and a deeper dip than that of the dimer with a nanorod in the same size, and accompanied by a red shift of the resonant wavelengths of the low-energy bonding plasmon modes. Besides, the structure-dependent Fano resonances of the trimer and their electric field distributions are shown in Fig. 8. It is found that the Fano resonances can be tuned by adjusting the positions of two nanorods situated in the sides of the nanoslice and the length of the nanorod. As shown in Fig. 8(a), when the position of nanorod g_1 decreases, the interaction of the dipole modes of nanoslice and nanorod increases, making the resonant peaks of the low-energy bonding plasmon modes red-shift, but the resonant peaks of the high-energy anti-bonding modes remain almost the same. In Fig. 8(b), the extinction spectra of the trimer change with varying nanorod length L_3, which demonstrated that Fano resonances of the trimer are still remaining for $L_3 \leq L_2$, but the high-energy anti-bonding modes in their extinction spectra are split into a quadrupole plasmon mode and an octupole plasmon mode for $L_3 > L_2$. This is because the dipole mode of the short nanorod ($L_3 < L_2$) only interacts with the quadrupole mode of the nanoslice, while the dipole mode of the long nanorod ($L_3 > L_2$) interacts with the quadrupole and octupole modes of the nanoslice so that

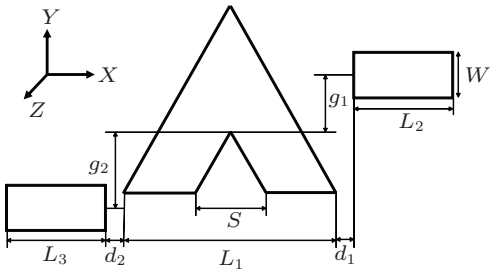


Fig. 6. The configuration of an Au triangle–rod trimer with geometric parameters: $L_1 = 130$ nm, $L_2 = 120$ nm, $L_3 = 120$ nm, $W = 60$ nm, $H = 30$ nm, and $S = L_1/3 = 43.3$ nm.

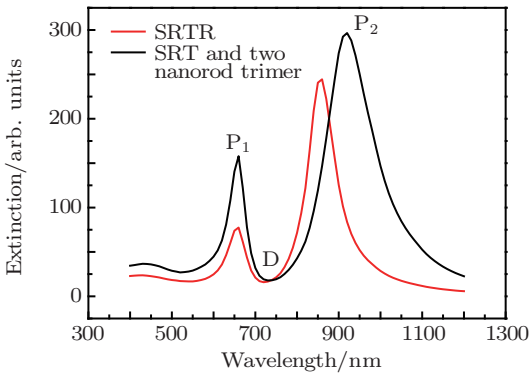


Fig. 7. The extinction spectrum of the proposed dimer and trimer for $d_1 = d_2 = 2$ nm and $g_1 = g_2 = 0$.

a split extinction spectrum is formed. It is obvious that the resonant wavelengths of the dipole and quadrupole plasmon modes of the trimer red-shift but the octupole plasmon modes are fixed when the lengths of left nanorod increase. Furthermore, we can see from Figs. 8(c) and 8(d) that the enhanced electric fields are mainly presented around the corners of nanorods for the resonant wavelength of the high-energy anti-bonding modes, and in two gaps between the two nanorods and the nanoslice for the resonant peaks of the low-energy bonding plasmon modes. Therefore, it is similar to the case of dimer that the strongest enhanced electric field is located in the gaps between the nanorods and the nanoslice.

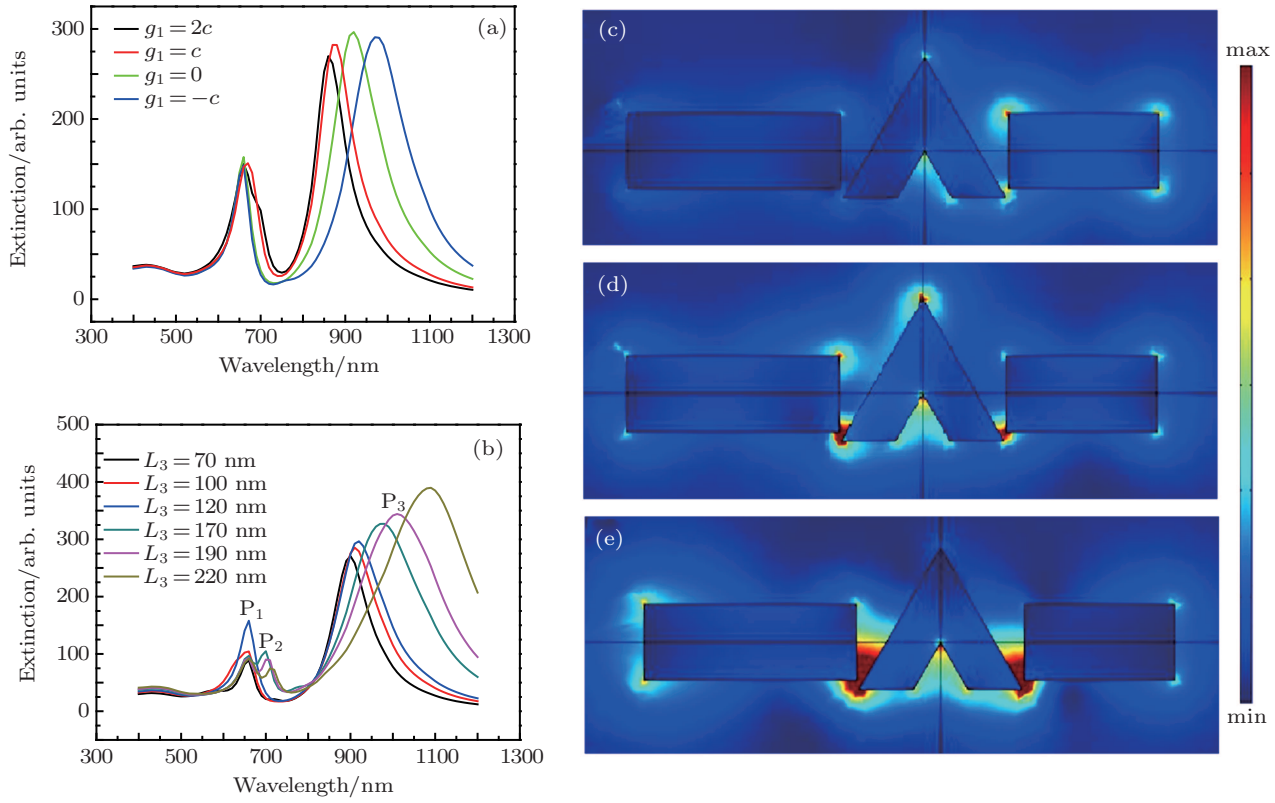


Fig. 8. The extinction spectra of the proposed trimer (a) for varying position of right nanorod g_1 at $d_1 = d_2 = 2$ nm and $g_2 = 0$ and (b) for varying length of left nanorod L_3 at $d_1 = d_2 = 2$ nm and $g_1 = g_2 = 0$. The electric field distributions at resonant peaks (c) P_1, (d) P_2, and (e) P_3, for $L_3 = 170$ nm, respectively. All the other structure parameters of the trimer are the same as those in Fig. 6.

4. Conclusion

A simple plasmonic gold triangle–rod dimer nanostructure consisting of a regular triangle nanoslice with a triangle split and a nanorod is proposed and its strong Fano resonance has been simulated by FEM. From the viewpoint of plasmon hybridization theory, the Fano resonance of the proposed nanosystem is the interference result between the "bright" dipole mode of the rod and the "bright" dipole and the "dark" quadrupole modes in the hybrid nanostructure, that is, the interaction among the plasmon modes leads to their coupling mode energy to be split into a high-energy anti-bonding mode and a low-energy bonding mode. The simulation results show that the extinction spectra of the dimer intensively depend on its geometric parameters. In particular, the resonant peak of low-energy bonding mode red-shifts but the resonant peak of high-energy anti-bonding mode blue-shifts with the decrease of the center offset or the coupling distance between the nanoslice and the nanorod. In addition, the intensities of Fano resonant peaks of the dimer are decreased with the increase of the polarization angle of incident light. Based on the dimer structure, a more perfect Fano resonance can be derived by a gold triangle–rod trimer nanosystem which simply adds another nanorod into the original dimer structure. The electric field distributions of the dimer and the trimer demonstrate an almost identical trend with varying of structure parameters, which reveals the same physics origin from the plasmonic hybridization or interference in the nano-assemblies. Our results are helpful to design a simple nanostructure with excellent performance of Fano resonance in the chemical and bio-sensing application.

References

[1] Krerbig U and Vollmer M 1995 *Optical Properties of Metal Clusters* (Berlin: Springer)

[2] Kelly K L, Coronado E, Zhao L L and Schatz G C 2003 *J. Phys. Chem. B* **107** 668

[3] Mulvaney P 1996 *Langmuir* **12** 788

[4] Jain P K, Huang X, EI-Sayed I H and EI-Sayed M A 2008 *Acc. Chem. Res.* **41** 1578
[5] Nordlander P, Oubre C, Prodan E, Li K and Stockman M I 2004 *Nano. Lett.* **5** 899
[6] Jana N R, Gearheart L and Murphy C J 2001 *Langmuir* **17** 6782
[7] Nikoobakht B and EI-Sayed M A 2003 *Chem. Mater.* **15** 1957
[8] Aizpurua J, Hanarp P, Sutherland D S, Kall M, Bryant G W and de Garcia A F J 2003 *Phys. Rev. Lett.* **90** 057401
[9] Liao Z W, Huang Y Z, Wang X Y, Chau I Y Y, Wang S X and Wen W J 2014 *Chin. Phys. Lett.* **31** 67803
[10] Hanarp P, Kall M and Sutherland D S 2003 *J. Phys. Chem.* **107** 5768
[11] Sherry L J, Chang S H, Schatz G C, van Duyne R P, Wiley B J and Xia Y 2005 *Nano. Lett.* **5** 2034
[12] Wang H, Wu Y, Lassiter B, Nehl C L, Hafner J H, Nordlander P and Halas N J 2006 *Proc. Natl. Acad. Sci. USA* **103** 10856
[13] Pena-Rodriguez O, Rivera A, Campoy-Quiles M and Pal U 2013 *Nanoscale* **5** 209
[14] Qian J, Li Y D, Chen J, Xu J J and Sun Q 2014 *J. Phys. Chem. C* **118** 8581
[15] Kottmann J and Martin O 2001 *Opt. Express* **8** 655
[16] Yang Z J, Zhang Z S, Hao Z H and Wang Q Q 2012 *Opt. Lett.* **37** 3675
[17] Verellen N, van Dorpe P, Vercruysse D, Vandenbosch G A and Moshchalkov V V 2011 *Opt. Express* **19** 11034
[18] Khan A D, Khan S D, Khan R, Ahmad N, Ali A, Khalil A and Khan F A 2014 *Plasmonics* **9** 1091
[19] Le F, Brandl D W, Urzhumov Y A, Aizpurua J and Nordlander P 2008 *ACS Nano* **2** 707
[20] Christ A, Solak H H, Gippius N A, Tikhodeev S G and Martin O J F 2007 *Phys. Rev. B* **76** 201405
[21] Christ A, Martin O J F, Einci Y, Gippius N A and Tikhodeev S G 2008 *Nano. Lett.* **8** 2171
[22] Yanchuk B L, Zheludev N I, Maier S A, Halas N J, Nordlander P, Giessen H and Chong C T 2010 *Nat. Mater.* **9** 707
[23] Ye J, Wen F, Sobhani H, Lassiter J B, van Dorpe P, Nordlander P and Halas N J 2012 *Nano. Lett.* **12** 1660
[24] Liu S, Yang Z, Liu R and Li X 2011 *J. Phys. Chem. C* **115** 24469
[25] Hao F, Sonnefraud Y, van Dorpe P, Maier S A, Halas N J and Nordlander P 2008 *Nano. Lett.* **8** 3983
[26] Zhang J, Xiao S, Jeppesen C, Kristensen A and Mortensen N A 2010 *Opt. Express* **18** 17187
[27] Chen J, Wang P, Chen C, Lu Y, Ming H and Zhan Q 2011 *Opt. Express* **19** 5970
[28] Zheludev N I, Prosvirnin S L, Papasimakis N and Fedotov V A 2008 *Nat. Photon.* **2** 351
[29] Yannopapas V, Paspalakis E and Vitanov N V 2009 *Phys. Rev. B* **80** 035104
[30] Sassan S, Young-wook J, Prashant K, Jain A and Paul A 2010 *Nano. Lett.* **10** 2655
[31] Shao L, Fang C H, Chen H J, Yat C M, Wang J F and Lin H Q 2012 *Nano. Lett.* **12** 1424
[32] Yun B F, Hu G H, Cong J W and Cui Y P 2014 *Plasmonics* **9** 691
[33] Habteyes T G, Dhuey S, Cabrini S, Schuck P J and Leone S R 2011 *Nano. Lett.* **11** 1819
[34] Yang D J, Yang Z J, Li Y Y, Zhou L, Hao Z H and Wang Q Q 2015 *Plasmonics* **10** 263
[35] Huo Y Y, Jia T Q, Zhang Y, Zhao H, Zhang S A, Feng D H and Sun Z R 2013 *Sensors* **13** 11350
[36] Wang W D, Li Y D, Peng J Y, Chen Z Q, Qian J, Chen J, Xu J J and Sun Q 2014 *J. Opt.* **16** 227
[37] Pena-Rodriguez O, Pal U, Campoy-Quiles M, Rodriguez-Fernandez L, Garriga M and Alonso M I 2011 *J. Phys. Chem. C* **115** 6410
[38] Contreras A M, Grunes J, Yan X M, Liddle A and Somorjai G A 2005 *Catalysis Lett.* **100** 115
[39] Johnson P B and Christy R W 1972 *Phys. Rev. B* **6** 4370
[40] Stratton J A 1941 *Electromagnetic Theory* (New York: McGraw-Hill) p. 206
[41] Brown L V, Sobhani H, Lassiter J B, Nordlander P and Halas N J 2010 *ACS Nano* **4** 819
[42] Butet J, Duboisset J, Bachelier G, Russier-Antoine I, Benichou E, Jonin C and Brevet P F 2010 *Nano Lett.* **10** 1717